CrossMark

ORIGINAL PAPER

Cerebellar Gray Matter Alterations in Huntington Disease: A Voxel-Based Morphometry Study

Paula C de Azevedo [1,2] (iD) · Rachel P Guimarães [1] · Camila C Piccinin [1] ·
Luiza G Piovesana [2] · Lidiane S Campos [2] · Juliana R Zuiani [2] · Eliza M. Tamashiro [3] ·
Giordanna Pinheiro [1] · Augusto C Amato-Filho [4] · Fernando Cendes [1,2] ·
Iscia Lopes-Cendes [5] · Anelyssa D'Abreu [1,2]

Abstract Neuropathological and neuroimaging studies in Huntington disease (HD) have suggested a role for the cerebellum. Our goal was to perform a detailed evaluation of cerebellar morphology. We performed the Unified HD rating scale (UHDRS) and Montreal cognitive assessment (MOCA) in 26 HD patients and 26 healthy controls. We created a two-sample test to analyze cerebellar gray matter (GM) differences between groups and another to correlate GM alterations with UHDRS and MOCA, corrected for age, expanded cytosine-adenine-guanine repeats, and disease duration using the spatially unbiased atlas template (SUIT)-SPM-toolbox which preserves anatomical detailing. We found increased GM density in the anterior cerebellum compared to controls. Higher GM density in the postero-superior lobe correlated with mood symptoms. Worse motor function and better cognitive function correlated with GM changes in the posterior cerebellum (false discovery rate (FDR) correction $p < 0.05$ and $k > 100$ voxels). In this detailed study of the in vivo cerebellar morphology in HD, we observed GM changes in regions involved in sensorimotor integration, motor planning, and emotional processing, supporting cerebellar involvement in the neuropathological process of HD.

Introduction

Huntington disease (HD) is an autosomal dominant neurodegenerative disorder caused by a cytosine-adenine-guanine (CAG) triplet expansion in the short arm of chromosome 4p16.3 in the Huntingtin (HT) gene. The expanded triplet with 36 repeats or greater confirms the molecular diagnosis of the disease [1]. In addition, there is an inverse relationship between the number of expanded triplet repeats with age of disease onset and the severity of clinical manifestations [2]. HD is a neuropsychiatric syndrome that includes motor, cognitive, and psychiatric symptoms, with chorea as the main motor manifestation [1].

Although symptoms have been largely explained by degeneration in the caudate, putamen, globus pallidus, thalamus, and amygdala [3, 4], cerebellar atrophy defined as a reduction of the cerebellar volume [5], is directly associated with psychiatric symptoms in the early phase of the disease [5–8]. Autopsy studies revealed atrophy of the paravermis and deep cerebellar nuclei [9–11]. In addition, it seems that cerebellar atrophy in the early stages of HD is independent of the degree of striatal degeneration [9].

The spatially unbiased atlas template (SUIT) is a spatially unbiased, high-resolution atlas template of the human cerebellum and brainstem, which maintains the anatomical detail of the cerebellar structures [12]. Our goal was to perform a detailed study of cerebellar morphology in HD, using the SUIT

✉ Paula C de Azevedo
paulacazevedo@yahoo.com.br

1. Neuroimaging Laboratory, University of Campinas UNICAMP, Campinas, Rua Vital Brasil, 251, Cidade Universitária Zeferino Vaz, Campinas, SP 13083-887, Brazil

2. Department of Neurology, University of Campinas UNICAMP, Campinas, SP 13083-887, Brazil

3. Department of Medical Psychology and Psychiatry, University of Campinas UNICAMP, Campinas, SP 13083-887, Brazil

4. Department of Radiology, University of Campinas UNICAMP, Campinas, SP 13083-887, Brazil

5. Department of Medical Genetics, University of Campinas UNICAMP, Campinas, SP 13083-887, Brazil

toolbox, and, secondarily, to perform a clinical-anatomical correlation.

Methods

Subjects The Institutional Review Board of our University Hospital approved the study and all subjects signed an informed consent. We recruited 26 right-handed patients (12 male; 49.42 ± 10.83 years) with molecularly confirmed HD (paternal and indeterminate inheritance were respectively 46.15 and 11.53%) and clinical signs of the disease from our neurogenetics outpatient clinic between 2013 and 2015. The mean age of symptom onset was 40.23 ± 9.79 years and mean expanded CAG repeat number was 42 ± 3.79. Exclusion criteria were a history of alcohol abuse, other previous or current neurologic and psychiatric disorders other than those related to the disease, major comorbidities, or contraindications to having magnetic resonance imaging (MRI). We also included 26 controls, perfectly matched for gender and age, without a personal or family history of neurological disorders and with a normal neurological examination.

Clinical Assessment We conducted interviews with subjects, family members, and caregivers, and also checked their CAG repeat size, professional and family history, environmental and drug exposure, medication, and clinical comorbidities. A neurologist expert in movement disorders performed a comprehensive neurologic examination and applied a specific clinical rating scale for HD—Unified Huntington disease rating scale (UHDRS), which includes motor and psychiatric evaluations, properly validated in Portuguese [13]. The UHDRS-motor assessment includes the examination of extrinsic ocular movement (ocular pursuit and saccades), dysarthria, tongue protrusion, dystonia, chorea, pull test, finger taps, pronate/supinate hands, Luria test ("fist-hand-palm"), rigidity, bradykinesia, gait, and tandem walking. Anxiety, sadness, low self-esteem/guilt, disruptive or aggressive behavior, irritable behavior, obsessions, compulsions, delusions, hallucinations, and suicidal thoughts are the psychiatric items of the UHDRS. The higher the score, the more severe the clinical picture in all UHDRS assessments. For cognitive assessment, we used the Montreal Cognitive Assessment (MOCA) [14].

MRI Acquisition Protocol Images were acquired on a 3 T Achieva MR unit-PHILIPS Intera®, release 2.6.1.0. In addition to the usual diagnostic sequences, we obtained volumetric T1-weighted images, with isotropic voxels of 1 mm3, acquired in the sagittal plane (1 mm thick, flip angle 8°, TR 7.1, TE3.2, matrix 240 × 240, and FOV 240 × 240 mm). An experienced neuroradiologist assessed all images, blindly, to rule out other neurological diseases and artifacts.

VBM-SUIT Tool The images were divided into patients and controls. Each subject was treated at the voxel-by-voxel level. The 3D–MRI images acquired in DICOM format were transformed to NIfTI (DCM2Nii software: http://www.mccauslandcenter.sc.edu/mricro/mricron/dcm2nii.html). In order to minimize any error, the images were aligned along the anterior commissure and rotated in sagittal, coronal, and axial planes. We used the SUIT tool (version 3.2), which isolates the infratentorial structures from surrounding tissue and generates targeted maps (gray matter (GM), white matter, and cerebrospinal fluid), providing a more accurate alignment between subjects than "whole-brain" methods (http://www.icn.ucl.ac.uk/motorcontrol/imaging/suit.htm). The SUIT tool classifies the cerebellar lobules more precisely than other VBM techniques [15–17]. The segmented GM images were normalized to the SUIT template. Then, we repositioned the generated maps to correct the variation of induced spatial normalization volume. Next, we conducted homogeneity tests using the images' covariance. Finally, the images were smoothed by a Gaussian filter kernel with 3 mm full-width half maximum (FWHM) contained in SPM12/Dartel (http://www.fil.ion.ucl.ac.uk) to satisfy the normal distribution assumed for statistical analysis of regional differences. The generated statistical parametric map identifies regions with significant differences in cerebellum.

Statistical Analysis Using SPM12, we created a two-sample test corrected for age for voxel-by-voxel analysis and detection of GM differences between the groups. A statistical parametric map was generated, which identified the cerebellar regions with significant differences. Initially, our statistical analyses were corrected for family wise error (FWE). However, the results using FWE were very conservative, therefore we utilized the false discovery rate (FDR) correction and reported the clusters with higher than 100 voxels (FDR $p < 0.05$, extent threshold $k \geq 100$ voxels), which is still a restricted analysis. Anatomical localizations of cerebellar lobules and vermis were determined by the probabilistic MRI atlas of human cerebellum by Diedrichsen et al. [18]. Secondly, to study the association between GM alterations and the UHDRS and MOCA scores, we performed a second t test corrected for age, disease duration, and CAG repeat number (FDR $p < 0.05$).

Results

We found GM density excess (FDR $p < 0.05$) in regions I–IV of the cerebellar lobes bilaterally compared to controls (Table 1 and Fig. 1). We observed GM density reduction (FDR $p < 0.05$) in regions VI on the right and V–VI on the left (Table 1 and Fig. 1).

Table 1 Results of VBM (SUIT tool) [12]

Size (voxels)	Localization
General analysis using FDR $p < 0.05$, $T = 3.25$ and $K > 100$ voxels	
GM excess regions	
378	Right I-IV
357	Left I-IV
GM decrease regions	
246	Right VI
143	Left V
121	Left VI

VBM voxel-based morphometry, *SUIT* spatially unbiased atlas template, *FDR* false discovery rate, *T* height threshold, *K* extent threshold, *GM* gray matter

Fig. 1 General analysis with the group differences in the GM density. *Green* regions demonstrating GM excess and purple regions the GM decrease. *GM* gray matter

We observed an association between the following clinical variables with GM density, adjusted for age, disease duration, and expanded CAG repeat number (Table 2 and Fig. 2):

1. UHDRS mood score: The mean score was 10 ± 7.55. Mood score was higher in subjects with higher GM density in region crus II on the right. In region VI on the left, the higher the mood scores, the lower the GM density.
2. UHDRS-motor score: The mean score was 21 ± 4.24. We found that the higher the GM density in vermis regions VIII and IX, the higher the motor scores. Whereas, the lower the GM density in crus I and II, IV, V, VI, VIIb, and VIII, at right, the greater the motor score.
3. MOCA score: The mean score was 22 ± 2.12. Subjects with higher cognitive scores had higher GM density in the left region VIII.

Discussion

This is one of the few studies which has detailed the in vivo cerebellar morphology in HD. The SUIT tool isolates the cerebellum from other brain structures providing a topographic detailing of each cerebellar lobe and assessing both GM increases and reductions. Most previous studies analyzed global cerebellar volume and found cerebellar atrophy in patients with HD [5, 9, 11, 19]. The present study specifically investigated cerebellar GM. We observed mostly GM excess in the anterior cerebellum, while GM was decreased mainly in the posterior cerebellum. It is important to point out that our findings do not exclude the possibility of coexistence of cerebellar atrophy with GM increase, which could be the result of white matter loss. As a secondary exploratory analysis, higher GM density in the postero-superior lobe was associated with mood disorder symptoms; worse motor function was associated with GM density alterations in the central portion of the postero-inferior lobe and lateral portion of the postero-superior lobe on
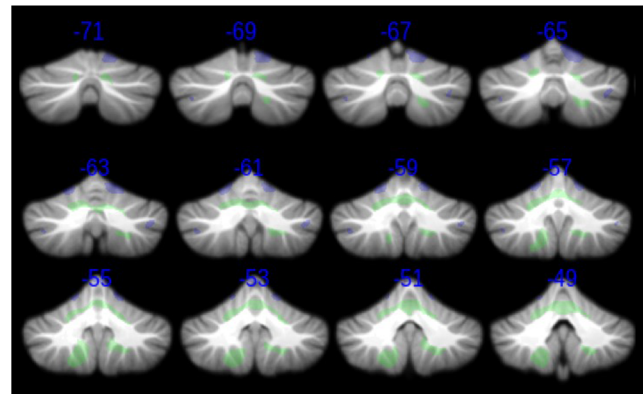
the right; and better cognitive function was with higher GM density in the left side of the postero-inferior lobe.

The GM density excess was found symmetrically in regions I–IV of the anterior cerebellar lobe. The subarea III, mainly lobule IV, is directly involved in upper limb motor control [20]. Gait and appendicular ataxia, dysarthria, as well as the control of tongue movements and orofacial muscles are directly related to the integrity of these regions [21].

We found GM density reduction mostly in areas VI of posterior cerebellar lobes bilaterally and V of anterior

Table 2 Results of clinical associations [12]

Size (voxels)	Localization
Clinical associations using FDR $p < 0.05$, $T = 3.59$ and $K > 100$ voxels	
Positive association: UHDRS-mood score and GM	
233	Right crus II
Negative association: UHDRS-mood score and GM	
119	Left VI
Positive association: UHDRS-motor score and GM	
315	Vermis VIII
191	Vermis IX
Negative association: UHDRS-motor score and GM	
383	Left VII b
197	Left VIII
393	Right crus II
382	Right VIII
368	Right VII b
334	Right crus I
401	Right IV/V
107	Right VI
201	Left VI
Positive association: MOCA score and GM	
247	Left VIII

FDR false discovery rate, *T* height threshold, *K* extent threshold, *GM* gray matter, *UHDRS* Unified Huntington disease rating scale, *MOCA* Montreal cognitive assessment
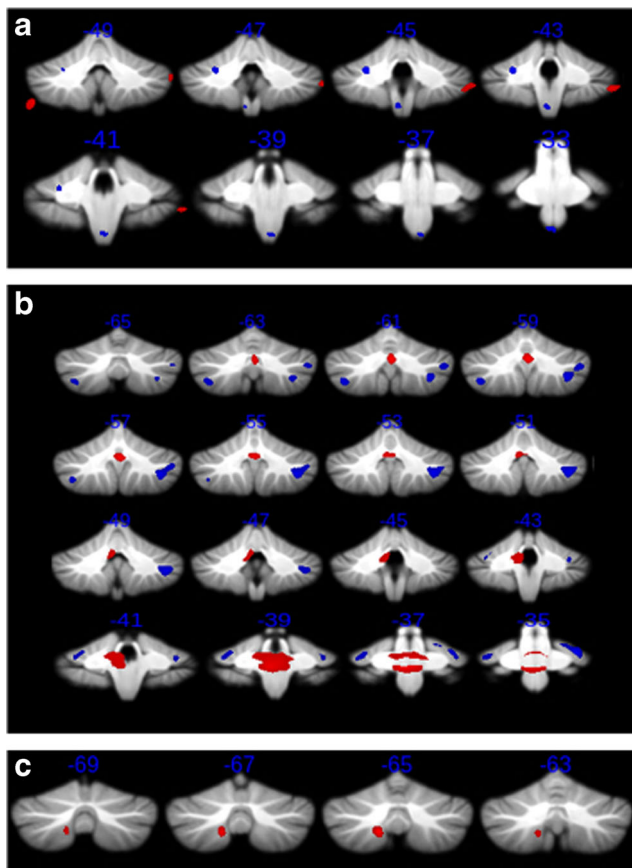
Fig. 2 Clinical associations and GM alterations. **a** Negative (*blue*) and positive (*red*) correlation between UHDRS-mood score and GM density; **b** Negative (*blue*) and positive (*red*) correlation between UHDRS-motor score and GM density; **c** Positive (*red*) correlation between MOCA score and GM density. *GM* gray matter; *UHDRS* Unified Huntington disease rating scale; *MOCA* Montreal cognitive assessment

none of those areas are primarily related to motor function, it is possible that they are markers of disease severity, or that there was some collinearity between motor and non-motor scores. Despite understanding atrophy and GM reduction is somehow intuitive, the relationship between increased GM density and mood symptoms is less clear, although this could be due to an adaptive or compensatory mechanism as discussed further below.

Higher motor scores were associated with lower GM density in a large cerebellar region: crus I and II, IV, V, VI, VIII, and VIIb on the right and VI, VIIb, and VIII on the left. These areas are involved in motor control (regions I–V, with a secondary representation in VIIIa/b lobules), multiple domain executive function (lobules VI and VII), saccades refinement, and sequential movements of hands (medially) and feet (laterally) (lobules VI and crus I), which include motor control and motor behavioral action [27, 28]. The ipsilateral somatotopic cerebellar representation justifies the right-sided predominance [27]. Together, those areas are responsible for fine motor control, more complex, and elaborate activities as well as sensorimotor learning.

Patients with higher MOCA scores had higher GM density in lobule VIII on the left, which is involved in sensorimotor tasks and working memory [27], suggesting a cerebellar role in cognitive dysfunction in HD.

Previous studies have also found GM excess in neurodegenerative diseases [15–17, 29]. There is no clear consensus between cortical thickness, GM volume, GM density, and neuropathological studies. In normal aging, the progressive frontal and temporal cortical thinning are not due to a reduction in neuronal counts but rather likely from a secondary loss of neuronal and dendritic architecture [30]. It is also speculated that the increase in GM observed during learning and practice-related tasks results from synaptic remodeling [31] and specific brain regions may change in either direction in response to environmental requirements [32]. Chorea is a hyperkinetic movement disorder, and it is not at all unlikely that the continuous movement and the required adaptations the patient is subject to in daily life may induce bidirectional GM increase in certain cerebellar areas.

The major limitation of our study was the small number of subjects and its transversal nature. Larger longitudinal samples may corroborate the clinical correlations observed and better characterize the cerebellar involvement. Currently, there is a consensus concerning a systems-level approach to the interplay between cerebellum, basal ganglia, and cortex [33]. The cerebellum targets multiple cortical areas and is reciprocally connected with the basal ganglia, indicating a subcortical densely interconnected network [33]. A more detailed clinical evaluation, with specific behaviors or movement disorders, may help uncover the interplay between cortex-thalamus-basal ganglia-cerebellum and the contribution of the cerebellum to motor and non-motor signs and symptoms.

cerebellar lobe on the left. Both are part of the sensorimotor cerebellum and are directly involved in learning and cognitive processing [22]. These areas are also indirectly attached to the prefrontal cortex through the dentate-rubral-thalamic tract, and the ventral portion of the dentate nucleus is the interface between those two areas [20].

Although mostly exploratory in nature, the clinical associations revealed some interesting results. UHDRS-mood scores were higher in subjects with lower GM density in region VI on the left, which is directly involved in processing empathy and perception of emotional intonation [22, 23] and higher GM density in region crus II on the right, which is connected to the posterior parietal and prefrontal cortices—limbic areas [24]. There was a positive association between UHDRS-motor score and the GM density in vermis areas VIII and IX, known as the limbic portion of the cerebellum because they are responsible for affective processing, and, with other posterior cerebellar regions, participate in higher cognitive tasks [25]. Structural posterior vermis lesions are the anatomical substrate of the cerebellar cognitive affective syndrome [26]. Since

Conclusion

In summary, we observed a pattern of cerebellar anatomical changes, which seemed to correlate to the motor, psychiatric, and cognitive manifestations of HD.

Author Roles
1- Research Project:
    a- Conception: Paula Christina de Azevedo; Anelyssa D'Abreu; Iscia Lopes-Cendes;
    b- Organization: Paula Christina de Azevedo; Anelyssa D'Abreu; Rachel Paes Guimarães; Iscia Lopes-Cendes;
    c-Execution: Paula Christina de Azevedo; Rachel Paes Guimarães; Camila C Callegari; Lidiane S Campos; Luiza G Piovesana; Juliana R. Zuiani; Eliza M. Tamashiro; Augusto C Amato-Filho;
 2- Statistical analysis:
    a- Design: Paula Christina de Azevedo; Anelyssa D'Abreu
    b- Execution: Paula Christina de Azevedo; Rachel Paes Guimarães;
    c- Review and critique: Anelyssa D'Abreu; Íscia Lopes-Cendes; Fernando Cendes
 3- Manuscript preparation:
    a- Writing of the first draft: Paula Christina de Azevedo; Anelyssa D'Abreu;
    Review and critique: Rachel P Guimarães; Camila C Callegari; Lidiane S Campos; Luiza G Piovesana; Juliana R. Zuiani; Eliza M. Tamashiro; Augusto C Amato-Filho; Fernando Cendes; Iscia Lopes-Cendes; Anelyssa D'Abreu.

References

1. Roos ACR. Huntington's disease: a clinical review. Orphanet J Rare Dis. 2010;5:40.
2. Stine OC, Pleasant N, Franz ML, Abbott MH, Folstein SE, Roos ACR. Correlation between the onset age of Huntington's disease and length of the trinucleotide repeat in IT-15. Hum Mol Genet. 1993;2(10):1547–9.
3. Bhide PG, Day M, Sapp E, Schwarz C, Sheth A, Kim J, Young AB, et al. Expression of normal and mutant huntingtin in the developing brain. J Neurosci. 1996;16:5523–35.
4. Sapp E, Schwarz C, Chase K, Bhide PG, Young AB, Penney J, et al. Huntingtin localization in brains of normal and Huntington's disease patients. Ann Neurol. 1997;42:604–12.
5. Rees EM, Farmer R, Cole JH, Haider S, Durr A, Landwehrmeyer B, Hobbs NZ, et al. Cerebellar abnormalities in Huntington's disease: a role in motor and psychiatric impairment? MovDisord. 2014;29(13):1648–54.
6. Lauterbach EC. Bipolar disorders, dystonia, and compulsion after dysfunction of the cerebellum, dentatorubrothalamic tract, and substantia nigra. Biol Psychiatry. 1996;40:726–30.
7. Kutty IN, Prendes JL. Psychosis and cerebellar degeneration. J Nerv Ment Dis. 1981;169:390–1.
8. Starkstein SE, Robinson RG, Berthier ML, Price TR. Depressive disorders following posterior circulation as compared with middle cerebral-artery infarcts. Brain. 1988;111:375–87.
9. Rüb U, Hoche F, Brunt ER, Heinsen H, Seidel K, Turco DD, et al. Degeneration of the cerebellum in Huntington's disease (HD): possible relevance for the clinical picture and potential gateway to pathological mechanisms of the disease process. Brain Pathol. 2013;23:165–77.
10. Jeste DV, Barban L, Parisi J. Reduced Purkinje cell density in Huntington's disease. ExpNeurol. 1984;85(1):78–86.
11. Rodda RA. Cerebellar atrophy in Huntington's disease. J Neurol Sci. 1981;50:147–57.
12. Diedrichsen J. A spatially unbiased atlas template of the human cerebellum. Neuro Image. 2006;33(1):127–38.
13. Tumas V, Camargos ST, Jalali PS, Galesso AP, Marques W Jr. Internal consistency of a Brazilian version of the unified Huntington's disease rating scale. Arquivos de Neuropsiquiatria. 2004;62(4):977–82.
14. Memória CM, Yassuda MS, Nakano EY, Forlenza OV. Brief screening for mild cognitive impairment: validation of the Brazilian version of the Montreal cognitive assessment. Int J Geriatr Psychiatry. 2013;28(1):34–40.
15. Piccinin CC, Santos MCA, Piovesana LG, Campos LS, Guimarães RP, Campos BM, et al. Infratentorial gray matter atrophy and excess in primary craniocervical dystonia. Parkinsonism Relat Disord. 2014;20:198–203.
16. Piccinin CC, Piovesana LG, Santos MCA, Guimarães RP, Campos LS, Campos BM, et al. Diffuse decreased gray matter in patients with idiopathic craniocervical dystonia: a voxel-based morphometry study. Front Neurol. 2015;5:283.
17. Guimarães RP, D'Abreu A, Yasuda CL, França MC Jr, Silva BHB, Cappabianco FAM, et al. A multimodal evaluation of microstructural white matter damage in spinocerebellar ataxia type 3. MovDisord. 2013;28(8):1125–32.
18. Diedrichsen J, Balster JH, Flavell J, Cussans E, Ramnani N. A probabilistic MR atlas of the human cerebellum. NeuroImage. 2009;46:39–16.
19. Fennema-Notestine C, Archibald SL, Jacobson MW, Corey-Bloom J, Paulsen JS, Peavy GM, et al. In vivo evidence of cerebellar atrophy and cerebral white matter loss in Huntington disease. Neurology. 2004;63(6):989–95.

20. Strick PL, Dum RP, Fiez JA. Cerebellum and nonmotor function. Annu Rev Neurosci. 2009;32:413–34.

21. Baloh R, Yee R, Honrubia V. Late cortical cerebellar atrophy. Brain. 1986;109:159–80.

22. Stoodley C, Schmahmann JD. Evidence for topographic organization in the cerebellum of motor control versus cognitive and affective processing. National Institute of Health Public Access. 2010;46(7):831–44.

23. Singer T, Seymour B, O'Doherty J, Kaube H, Dolan R, Frith C. Empathy for pain involves the affective but not sensory components of pain. Science. 2004;303:1157–62.

24. Kelly R, Strick P. Cerebellar loops with motor cortex and prefrontal cortex. J Neurosci. 2003;23:8432–44.

25. Bobee S, Mariette E, Tremblay-Leveau H, Caston L. Effects of early midline cerebellar lesion on cognitive and emotional functions in the rat. Behav Brain Res. 2000;112:107–17.

26. Schmahmann JD, Sherman JC. The cerebellar cognitive affective syndrome. Brain. 1998;121:561–79.

27. Stoodley CJ, Schmahmann JD. Functional topography in the human cerebellum: a meta-analysis of neuroimaging studies. Neuro Image. 2009a;44:489–501.

28. Schlerf J, Wiestler T, Verstynen T, Diedrichsen J. Big challenges from the "Little Brain"—imaging the cerebellum. Advanced Brain Neuroimaging Topics in Health and Disease-Methods and Applications. 2014(8):199–223.

29. Keller SS, Mackay CE, Barrick TR, Wieshmann UC, Howard MA, Roberts N. Voxel-based morphometric comparison of hippocampal and extrahippocampal abnormalities in patients with left and right hippocampal atrophy. NeuroImage. 2002;16(1):23–31.

30. Freeman SH, Kandel R, Cruz L, Rozkalne A, Newell K, Frosch MP, Hedley-Whyte ET, Locascio JJ, Lipsitz LA, Hyman BT. Preservation of neuronal number despite age-related cortical brain atrophy in elderly subjects without Alzheimer disease. J Neuropathol Exp Neurol. 2008;67(12):1205–12.

31. Ilg R, Wohlschäger AM, Gaser C, Liebau Y, Dauner R, Wöller A, Zimmer C, Zihl J, Mühlau M. Gray matter increase induced by practice correlates with task-specific activation: a combined functional and morphometric magnetic resonance imaging study. J Neurosci. 2008;28(16):4210–5.

32. Lerch JP, Yiu AP, Martinez-Canabal A, Pekar T, Bohbot VD, Frankland PW, Henkelman RM, Josselyn SA, Sled JG. Maze training in mices induces MRI-detectable brain shape changes specific to the type of learning. NeuroImage. 2011;54(3):2086–95.

33. Caligiore D, Pezzulo G, Baldassarre G, Bostan AC, Strick PL, Doya K, et al. Consensus paper: towards a systems-level view of cerebellar function: the interplay between cerebellum, basal ganglia, and cortex. Cerebellum. 2017;16(1):203–229.